

Nonlinear effects in dipole solvation. II. Optical spectra and electron transfer activation

Dmitry V. Matyushov and Branka M. Ladanyi

Department of Chemistry, Colorado State University, Fort Collins, Colorado 80523

(Received 15 August 1996; accepted 23 April 1997)

We present a theoretical analysis of the effect of nonlinear dipole solvation on steady-state optical spectra and intramolecular electron transfer (ET) reactions. The solvation nonlinearity is attributed to saturation of a dipolar liquid produced by the solute dipole. The treatment explores the perturbation expansion over the solute-solvent dipolar interaction truncated in the form of a Padé approximant. The optical line shape and the free energies along the ET reaction coordinate are related to the chemical potential of solvation of a fictitious solute with a complex-valued dipole moment. Due to solvent dipolar saturation the spectrum of dipolar fluctuations is confined by a band of the width $2E_{\text{lim}}$. Solvation nonlinearity was found to manifest itself for optical transitions with high dipole moments in the initial state, most often encountered for emission lines. In this case, the spectral line approaches the saturation boundary E_{lim} bringing about "line squeezing" and decrease of the line shift compared to the linear response prediction. In the nonlinear region, the line shift dependence on the solute dipole variation Δm switches from the quadratic linear response form $\propto \Delta m^2$ to a linear trend $\propto |\Delta m|$. The bandwidth may pass through a maximum as a function of $|\Delta m|$ in the saturation region. Nonlinear solvation results thus in a narrowing of spectral lines. For a transition with solute dipole enhancement, the bandwidth in emission Δ_e is therefore lower than in absorption Δ_a : $\Delta_e < \Delta_a$. As a result, the plot of $\beta\Delta_{a,e}^2$, $\beta = 1/k_B T$ against the Stokes shift $\hbar\Delta_{st}$ demonstrates the upward deviation of $\beta\Delta_a^2$ and downward deviation of $\beta\Delta_e^2$ from the linear response equality $\beta\Delta_{a,e}^2 = \hbar\Delta_{st}$. We also explored the nonlinearity effect on charge separation/charge recombination activation thermodynamics. The solvent reorganization energy was found to be higher for charge separation (λ_1) than for charge recombination (λ_2). Both are smaller than the linear response result. For the reorganization energies, the discrepancy between λ_1 and λ_2 is relatively small, whereas their temperature derivatives deviate significantly from each other. The theory predictions are tested on spectroscopic computer simulations and experiment. Generally good quantitative agreement is achieved. © 1997 American Institute of Physics. [S0021-9606(97)01529-8]

I. INTRODUCTION

The inhomogeneous broadening and shift of optical spectral lines induced by a condensed phase environment are fundamental properties characterizing the solvation power of the medium. Based on this viewpoint, optical spectral dyes are widely used as microscopic probes of solvent polarity.^{1,2} Activation parameters of electron transfer (ET) reactions are available from the bandshape analysis of ET optical spectra^{3,4} rendering the two fields of optical spectroscopy and ET reactions progressively more closely allied. Both problems are therefore treated here in the framework of the common formalism of Padé truncation of the perturbation expansion for the solvation chemical potential developed in the preceding paper⁵ (paper I).

In spectroscopic measurements, the chromophore dipole moment varies due to optical transition from the ground state value m_g to the excited state dipole m_e . Differential solvation of the excited (nonequilibrium) and ground (equilibrium) dipolar states leads to a spectral shift probing the electrostatic potential created by the solvent at the solute location. In the widely used linear response approximation (LRA)^{6,7} the local solute potential is assumed to be proportional to the solute dipole moment m_0 resulting in a solvation

chemical potential μ_p scaled by the squared solute dipole moment $\mu_p = -am_0^2$. The proportionality coefficient a termed the response function is factored for large solutes into the solute size and solvent components. For the continuum solvent response, they are the cube of the inverse solute radius and the dielectric function $(\epsilon - 1)/(2\epsilon + 1)$, where ϵ is the solvent dielectric constant. It is therefore the LRA that forms the background of using optical chromophores as solvent polarity indicators. Deviations from linear response would manifest themselves as a dependence of the response function on the solute dipole moment.

In the LRA, the spectral shift and width are no longer independent.⁸ The difference of the absorption and emission energies $\hbar\Delta_{st}$ (Stokes shift) is related to the spectral width Δ by the formula

$$\hbar\Delta_{st} = \beta\Delta^2, \quad (1)$$

where $\beta = 1/k_B T$. This relation is often used⁹ as a critical test of the LRA applicability. Physically, the LRA is valid provided the solute-solvent interaction is weaker than solvent-solvent coupling, thus imposing only a small perturbation on the liquid. In practice, however, the desire for achieving well-resolved solvent-induced shifts leads to the use of chro-

mophores with high dipole moment variations $\Delta m = m_e - m_g$ for which the LRA ansatz may break down. This raises the question of the range of applicability of the LRA and the relative impact of nonlinear solvation.

The problem of nonlinear effects in equilibrium^{10–16} and nonequilibrium^{17–19} solvation, especially of ions, has already a long history. Numerous simulations have been performed to test the solute charge dependence of the ion solvation free energy. Although the response function was found to be generally dependent on the sign of the charge, the quadratic ion charge dependence of the solvation free energy has been reasonably well reproduced in the majority of studies. The sign-dependence of the response function was related to the asymmetry of the intramolecular charge distribution in solvent molecules^{10,15,16} or to specific force effects. The conclusion that can be drawn is that the average potential of the solvent is approximately linear in the solute charge in the charge range explored. This effect is due to the compensation between the orientational saturation in the first solvation shell and the closer approach of the solvent molecules to a charged solute.^{15,16,20} The nonlinear aspect of charge solvation manifests itself, however, in the fluctuation $\langle \delta V^2 \rangle$ of the solvent potential V . The “freezing” of the solvent induced by a charged solute leads to the approximately quadratic^{15,21} increase of the force constant $k_V \equiv k_B T / \langle \delta V^2 \rangle$ with the solute charge. The Gaussian distribution of the potential fluctuations thus becomes narrowed due to nonlinear saturation effects.

The nonlinear effects in dipolar solvation have been much less explored than those of the ionic solute case. Yet they may be even more pronounced for dipolar solutes. The clue to this suggestion is provided by the comparison of the solvation energies of ions and dipoles obtained as a first order perturbation over the solute-solvent potential. The linear response solvation energy of an ion contains only the longitudinal solvent response $\propto (1 - 1/\epsilon)$ finite even in the infinite polarity limit $\epsilon \rightarrow \infty$. On the other hand, the solvent response to a dipolar solute is a linear combination of the longitudinal and transverse response functions²² (see also paper I). The latter $\propto (\epsilon - 1)$ diverges at $\epsilon \rightarrow \infty$ indicating violation of the LRA. In continuum and integral equation theories this difficulty is overcome by incorporating the self-consistency through the reaction field concept in the former case and by summing the chain solvent dipole-dipole diagrams in the latter. However, the very existence of this singularity may signal the possibility of nonlinear effects in dipole solvation more pronounced than those of ionic solutes. This conjecture is actually borne out by very recent simulations of ion and dipole hydration²³ where the linear response approximation was found to be less accurate for dipolar than for ionic solutes.

Concerning dipole solvation, molecular dynamics computer simulations have chiefly been performed on a physically related system of a rigid diatomic of oppositely charged spherical sites. Several nonlinear solvation effects have been observed for such ion pair solutes. Carter and Hynes¹⁷ find a substantial narrowing of the time dependent fluorescence lines when a charge separated state has been created in a

polar fluid modeling methyl chloride. Fonseca and Ladanyi¹⁸ observed marked departure from the linear response expectations when studying the solvation dynamics in methanol. Further detailed studies¹⁹ have shown that the effect is to be attributed to nonlinear response of the solute-solvent hydrogen bonding to the change in the charge of the solute site. On the other hand, studies of the dynamic solvent response to an instantaneously created solute dipole have clearly shown^{15,24,25} that without specific solute-solvent interactions the deviations from linear response behavior are relatively small. In spite of these recent findings encouraging the application of the LRA in steady state spectroscopy and intramolecular ET reactions, some fundamental questions remain open. First, it is still unclear what are the general conditions of applicability of the LRA and how they are affected by the solute and solvent properties. Second, the results obtained for the instantaneously created dipole may not hold for the states with nonzero initial dipole moments. The latter point concerns especially emission spectra (or absorption of negative chromophores²) characterized by high values of the initial state dipole moment. Notice in this respect the contradiction between the results obtained for the fluorescence of the charge transfer state¹⁷ where nonlinear effects were clearly seen and those for the instantaneously created dipole^{15,24,25} where they have not been found. Let us consider this point more closely.

Due to thermal fluctuations of the polar liquid the solute initial and final electronic states acquire a distribution of energy levels. The maximum of the spectral line is just the first moment of this distribution. The scanned light frequency probes different parts of the distribution of levels with nonequilibrium energies produced by solvent fluctuations. The energy of creating such a fluctuation can be treated as a solvation energy of some fictitious solute dipole.²⁶ If the initial (e.g., emission) state already possesses a high dipole moment, the real and fictitious dipoles add up. The wings of the spectral line can thus be characterized by large effective solute dipoles for which nonlinear solvation effects may assume significance resulting in deviation from Gaussian behavior. This is indeed the picture observed in the present work. Due to nonlinear solvation effects the emission spectral lines get squeezed resulting in a line narrowing.

If nonlinear solvation manifests itself in steady state spectroscopy, the important question is which of its consequences could be recognized in experiments. The violation of the linear response relation (1) is commonly considered as the main indicator of nonlinear solvation effects. However, as we show below, this is not the only manifestation of nonlinear solvation. Therefore, our attention in the present work is chiefly focused on qualitative consequences of nonlinear dipolar solvation for the solvent-induced shifts and widths of optical spectral lines. To this end, we consider here the simple model of a spherical solute in a dipolar solvent of spherical nonpolarizable molecules with centered point dipoles. Our restriction to a nonpolarizable fluid is motivated by the existence in this case of a simple connection between the spectral shape and the chemical potential of solvation of a fictitious solute with a complex-valued dipole moment, as

suggested by Loring.^{27,28} In fact, an analogous representation exists also for polarizable nonpolar liquids,^{29,30} but the situation becomes more complicated when both polarizability and permanent dipole moments are involved. Although the role of the solute and solvent polarizabilities is increasingly appreciated in present-day studies of equilibrium³¹ and nonequilibrium^{25,32,33} solvation phenomena, these also clearly indicate that the qualitative results obtained for purely dipolar fluids remain largely intact when the solvent polarizability is included. Therefore, the nonpolarizable model seems to be sufficient to clarify the general features of nonlinear effects due to the dipolar component of solvation. Such a model is obviously inadequate for treating optical spectra and ET reactions in weakly polar and nonpolar solvents where induction²⁹ and dispersion^{30,34–37} forces caused by the solute and solvent polarizabilities as well as higher multipoles^{38,39} play a significant role.

The issue of nonlinear solvation effects in ET reactions has continuously been attracting attention during several decades.^{33,38,40–43} Following the treatment of Kakitani and Mataga (for a recent review see Ref. 41) the studies of nonlinear effects focused chiefly on the energy gap dependence of ET rates. Unfortunately, the dependence of the ET rate on the energy gap is strongly affected by the solute intramolecular vibrational excitations for intramolecular ET^{3,4,44} and, in addition, by the distribution of reaction distances for outer sphere ET.^{41,45} Furthermore, the experimental accuracy does not make it possible to distinguish clearly between different factors determining the ET energy gap law.⁴¹ Spectroscopic data seem to be more reliable for treating nonlinear effects and we suggest below a test of nonlinear solvation effects on ET involving the comparison of charge separation vs charge recombination reorganization energies and entropies.

The remainder of the paper is organized as follows. In Sec. II we derive the analytical expression for the line shape using the Padé form of the chemical potential of dipole solvation. The dependencies of the linewidth and shift on the solute dipole moment are analyzed. The role of nonlinear solvation in intramolecular ET reactions is considered in Sec. III. The comparison to simulations and experiment is the subject of Sec. IV. Finally, we conclude in Sec. V by summarizing our main results.

II. LINE SHAPE CALCULATION

The intensity $I_a(\omega)$ of the absorption spectral line caused by the solute dipole optical transition $\mathbf{m}_g \rightarrow \mathbf{m}_e$, $\Delta \mathbf{m} = \mathbf{m}_e - \mathbf{m}_g$ in a chromophore in a dipolar liquid can be expressed in terms of the chemical potential μ_p of solvation of a fictitious complex-valued dipole according to the relation²⁷

$$I_a(\omega) = \int_{-\infty}^{\infty} \frac{ds}{2\pi} \exp(-is\beta\Delta E) C(s), \quad (2)$$

where $\Delta E = \hbar(\Omega - \omega)$ is the deviation of the transition energy from the vacuum value $\hbar\Omega$ and

$$C(s) = \exp[-\beta\mu_p(\mathbf{m}_g + is\Delta \mathbf{m}) + \beta\mu_p(\mathbf{m}_g)]. \quad (3)$$

The emission intensity can be obtained analogously after the replacement $\mathbf{m}_g \rightarrow \mathbf{m}_e$ and $\Delta \mathbf{m} \rightarrow -\Delta \mathbf{m}$.

The chemical potential difference under the exponent in Eq. (3) determines the free energy of creating a nonequilibrium solvent fluctuation corresponding to an equilibrium configuration with some effective solute dipole moment the magnitude of which is determined by the energy gap ΔE . Since the spectral intensity at some particular value of ΔE is a statistically weighted sum over all such fluctuations, we get the integral over the imaginary part of the solute dipole. In order to evaluate it correctly we need an expression for the solvation chemical potential valid in the whole range of effective dipole moments $|\mathbf{m}_g + is\Delta \mathbf{m}|$. Unfortunately, most of the molecular treatments of dipolar solvation involve the LRA or, when nonlinear, can be used only in a very limited range of solute dipoles and are not easily extendable to the complex plane of solute dipoles. Additionally, the complicated nature of calculations in molecular theories involving nonlinearity like the hypernetted-chain approximation⁴⁶ makes them difficult to use in spectral line and ET calculations. That is why we developed in the preceding paper⁵ an alternative approach based on the Padé truncation of the perturbation expansion of the solvation chemical potential over the dipole-dipole solute-solvent interaction. Apart from its simplicity, the Padé form of the solvation chemical potential is analytically extendable into the complex plane of solute dipole moments making it applicable to spectral line shape calculations.

The Padé truncation of the perturbation expansion for a spherical solute of radius R_0 results in the expression for the solvation potential in the form

$$-\mu_p(m_0) = \frac{a(y, \rho^*, r_{0s})m_0^2}{1 + b(y, \rho^*, r_{0s})m_0^2}, \quad (4)$$

which reproduces the quadratic linear response dependence on the solute dipole moment m_0 at small m_0 magnitudes and includes dipolar saturation $\mu_p \rightarrow -a/b$ at $m_0^2 \gg 1/b$. The expansion coefficients in Eq. (4) are functions of the polarity parameter $y = (4\pi/9)\beta\rho m^2$, the reduced solvent density $\rho^* = \rho\sigma^3$, and the distance of the closest approach of the solvent molecules to the solute $R_{0s} = R_0 + \sigma/2$, $r_{0s} = R_{0s}/\sigma$, where σ is the solvent hard sphere (HS) diameter. The explicit relations for the coefficients $a(y, r_{0s})$ and $b(y, r_{0s})$ in Eq. (4) are given in paper I.

Equation (4) can now be used in Eqs. (2) and (3) to calculate the spectral line shape. If we restrict ourselves only to the linear response term, we get the familiar Gaussian form

$$I_a^{(l)}(\omega) = (2|\Delta \mathbf{m}| \sqrt{\pi\beta a})^{-1} \exp\left(-\beta \frac{(\Delta E - \delta_a^{(l)})^2}{4a\Delta m^2}\right), \quad (5)$$

where the shift of the absorption line relative to the gas phase transition is

$$\delta_a^{(l)} = 2a\mathbf{m}_g \cdot \Delta \mathbf{m}. \quad (6)$$

The integration in Eq. (3) with the nonlinear solvation potential (4) can be performed in the steepest descent approximation. In this way, the value of the integral is determined by the value of the function under the exponent

$$\mathcal{F}(s) = -is\beta\Delta E + \beta a(\mathbf{m}_g + is\Delta\mathbf{m})^2 / [1 + b(\mathbf{m}_g + is\Delta\mathbf{m})^2], \quad (7)$$

at the stationary point s^\ddagger such that $\mathcal{F}'(s^\ddagger) = 0$. This condition gives the effective solute transition dipole $\mathbf{m}^\ddagger = \mathbf{m}_g + is^\ddagger\Delta\mathbf{m}$ at which the transition occurs. It is determined by the relation

$$\frac{\mathbf{m}^\ddagger}{(1 + b\mathbf{m}^{\ddagger 2})^2} = \frac{\Delta E \Delta\mathbf{m}}{2a\Delta m^2}. \quad (8)$$

The most important observation from Eq. (8) is that the region of the existence of the stationary point s^\ddagger is limited by the range of the energy gap magnitudes

$$|\Delta E| < E_{\text{lim}} = 9a|\Delta m| / (8\sqrt{3}b). \quad (9)$$

This relation confines the range of the permissible effective dipoles $m^\ddagger < 1/\sqrt{3}b$ for which the second derivative of $\mathcal{F}(s)$ at the stationary point

$$\mathcal{F}''(s)|_{m^\ddagger} = -2a\beta|\Delta m| \frac{(1 - 3bm^{\ddagger 2})}{(1 + bm^{\ddagger 2})^2}$$

remains negative. For the frequencies that violate the inequality (9) the line intensity should be set equal to zero. This is the mathematical reflection of the involvement of solvent saturation. Physically it implies that a dipolar liquid cannot create a dipolar fluctuation of infinite energy and the range of accessible energy fluctuations is confined by the band $-E_{\text{lim}} < \Delta E < E_{\text{lim}}$. The boundaries of this band restrict in turn the range of frequencies with nonzero absorption intensities. It is clear that nonlinear solvation effects can manifest themselves when the energy ΔE approaches the limits $\pm E_{\text{lim}}$. By contrast, in the center of this interval the linear response approximation should hold. This point explains why no significant deviations from the linear response behavior have been observed for an instantaneously created dipole in nonprotic polar solvents.^{15,24} In this case, the absorption maximum is positioned at $\Delta E = 0$ and the line intensity decays almost to zero at the boundaries $\pm E_{\text{lim}}$. Actually, we have not found any noticeable discrepancies in absorption ($m_g \rightarrow m_e$, $m_g = 0$) line shape between the linear response limit $I_a^{(l)}(\omega)$ and the nonlinear result

$$I_a^{(n)}(\omega) = (2|\Delta m|D\sqrt{\pi\beta a})^{-1} \times \exp\left(-\beta \frac{am^{\ddagger 2}(1 - bm^{\ddagger 2})}{(1 + bm^{\ddagger 2})^2} + 2\beta \frac{a\mathbf{m}^\ddagger \cdot \mathbf{m}_g}{(1 + bm^{\ddagger 2})^2} - \beta \frac{am_g^2}{1 + bm_g^2}\right), \quad (10)$$

$$D = (1 - 3bm^{\ddagger 2})^{1/2} / (1 + bm^{\ddagger 2})$$

obtained in the steepest descent approximation with m^\ddagger from Eq. (8). The calculations have been performed for two dipole

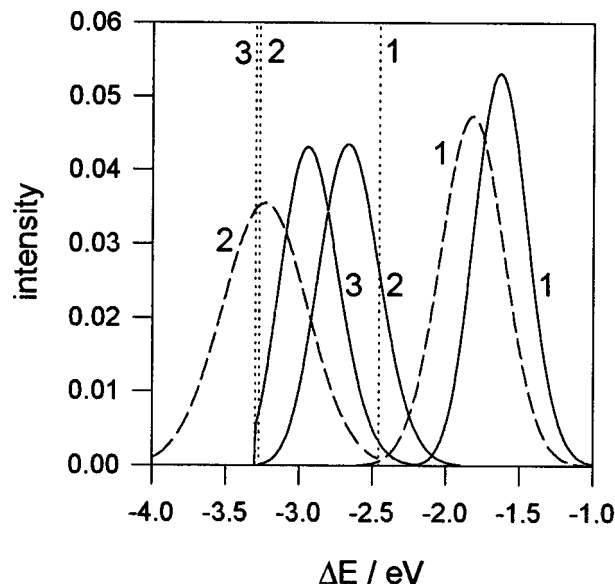


FIG. 1. Linear (dashed lines) and nonlinear (solid lines) response emission lines in methanol (1,2) and acetonitrile (3) corresponding to the emission transition $m_e \rightarrow 0$ with $m_e = 15$ D (1) and 20 D (2,3). Solute size is $R_0 = 4$ Å. The dotted lines show the dipolar fluctuation boundaries E_{lim} . The solvent parameters are $\sigma = 3.77$ Å, $\rho^* = 0.793$, $m = 2.34$ D (1,2) and $\sigma = 4.14$ Å, $\rho^* = 0.810$, $m = 4.3$ D (3).

lar liquids modeling methanol^{47,48} ($\sigma = 3.77$ Å,⁴⁹ $\rho^* = 0.793$, and $m = 2.34$ D) and acetonitrile⁵⁰ ($\sigma = 4.14$ Å, $\rho^* = 0.810$, and $m = 4.3$ D). The solvent permanent dipole moments have been slightly increased compared to the gas phase value $m = 1.70$ D for methanol and $m = 3.50$ D for acetonitrile to accommodate the effect of the solvent polarizability enhancing the average solvent dipole moment. For the solute, the radius $R_0 = 4$ Å common for spectroscopic applications has been used.

For the adopted parameters we found that relations (5) and (10) coincide almost exactly with the integral (2) invoking μ_p from Eq. (4) for the absorption transition $0 \rightarrow \Delta\mathbf{m}$ with Δm in the range $0 \leq \Delta m \leq 20$ D. However, the situation changes dramatically for emission transitions for which the chromophore has already an appreciable dipole moment in the equilibrium excited state. (The same is true for absorption lines with high magnitudes of m_g , e.g., for negative chromophores.²) Let us consider the emission transition $\Delta\mathbf{m} \rightarrow 0$, $\mathbf{m}_e = \Delta\mathbf{m}$. The maximum of the emission line shifts progressively with increasing Δm . For relatively small Δm magnitudes, the nonlinear line shift $\delta_e^{(n)}$ is proportional to Δm^2 according to the linear response prediction (6). With increasing Δm the maximum approaches the fluctuation band boundary E_{lim} (Fig. 1). This results in two major effects: (i) the line narrows (Fig. 2) and (ii) the quadratic $\delta_e^{(n)} \propto \Delta m^2$ emission shift variation switches to the linear dependence $\delta_e^{(n)} \propto \Delta m$ (Fig. 3). We consider both effects separately below.

As is illustrated in Fig. 1, the emission line is cut off from the side of the boundary $-E_{\text{lim}}$ for large Δm magnitudes and strong solvent polarities. For our example, noticeable cut-off of the line is observed only for a high Δm value

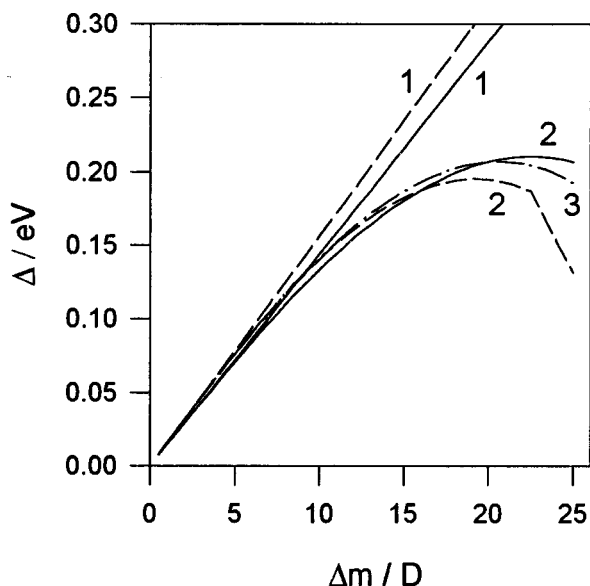


FIG. 2. Bandwidth of the emission transition $m_e \rightarrow 0$ vs the solute dipole moment change $\Delta m = m_e$ for the linear (1) and nonlinear (2,3) responses in methanol (solid lines) and acetonitrile (dashed lines). The curves labeled by 2 refer to the width definition according to Eq. (11); 3 represents the width obtained by replacing $\Delta(1/2)$ in Eq. (11) by the twice distance from the maximum position to the right line wing on the half intensity level. The solute size is $R_0 = 4 \text{ \AA}$, the solvent parameters are as in Fig. 1.

in acetonitrile as the solvent. Since this nonlinear effect produces a deviation of the line shape from the Gaussian form, the line width can be determined according to the experimentally widely accepted definition

$$\Delta = \Delta(1/2)/(8\ln 2)^{1/2} \quad (11)$$

through the half-intensity width $\Delta(1/2)$. Even before the half-intensity level reaches the boundary $-E_{\text{lim}}$, the line narrows (Fig. 2) compared to the linear response prediction

$$\Delta^{(l)} = \sqrt{2a/\beta} |\Delta m|.$$

Ultimately, when the half-width level reaches the boundary $-E_{\text{lim}}$, the width begins to decrease sharply (curve 2 in Fig. 2). The total dependence of the linewidth on Δm passes through a maximum. The decaying branch of the curve could be referred to the specific definition of the width according to Eq. (11). However, if we consider only the right spectral wing and define the width as twice the distance from the maximum position to the right emission wing at the half intensity level, we also obtain a maximum (curve 3, Fig. 2). This indicates that restrictions imposed by the solute on the solvent molecules diminish thermal orientational fluctuations of the permanent dipoles and the emission line becomes nonlinearly narrowed. The bandwidth maximum appears, however, only at very high (taking into account the relatively small chromophore size) values of the excited state dipole moment. For common chromophores it can hardly be observed and only the line narrowing compared to the linear response width should be expected. On the other hand, clearly analogous nonlinear narrowing has recently been obtained by Chong and Hirata.⁵¹ They calculated first three

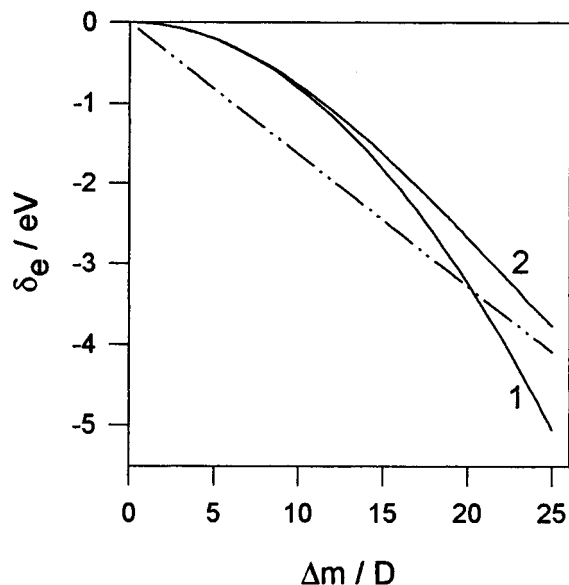


FIG. 3. Emission shift vs the solute dipole moment change obtained for the linear (1) and nonlinear (2) responses in methanol. The dash-dotted line shows the dipolar fluctuations band limit E_{lim} . The solute and solvent parameters are as in Fig. 2.

moments of the solute-solvent potential in the framework of the extended reference interaction site method. The solutes studied were monatomic ions A^q and neutral diatomics A^q-B^{-q} with the varying charge q . For both solutes in a dipolar liquid the second cumulant of the solute-solvent potential was found to pass through a maximum in a fashion very similar to that depicted in Fig. 2. Furthermore, for the dipolar solute, the magnitude of the solute dipole at the maximum $\Delta m \approx 25 \text{ D}$ falls in the range obtained in the present study (see Fig. 2).

Of course, the cut-off of the emission line at the $-E_{\text{lim}}$ boundary as that shown in Fig. 1 will be smoothed for real systems by the influence of other solvent and solute modes. From the latter, the intramolecular solute vibrations assume particular importance for large negative ΔE values. However, the existence of the energetic boundary $-E_{\text{lim}}$ for the dipolar liquid fluctuations may affect the results of the line shape analysis permitting one to extract spectroscopic characteristics and activation parameters crucial for intramolecular ET reactions.^{3,4}

Nonlinear narrowing of emission lines analogous to that reported here has been observed by Carter and Hynes¹⁷ in ion-pair simulations. The effect was attributed to the decrease of the force constant of solvent fluctuations induced by the solute. That picture is consistent with the proposal of Kakitani and Mataga (KM)²¹ who claimed that restrictions on the solvent molecules imposed by a charged solute should increase the curvature of the Gaussian distribution of the solvent potential magnitudes. This point deserves special comment. As can be easily seen from comparing Eqs. (5) and (10), the curvatures of linear and nonlinear spectral lines at the maximum are the same. The spectral narrowing is in fact produced by the deviation of the line shape from the Gaussian form when approaching $\pm E_{\text{lim}}$ boundaries and not

by the variation of parabolic force constants. Only when fitted to a parabola, does the nonlinear spectral line correspond to an effectively Gaussian medium with a diminished force constant of solvent fluctuations. This picture is analogous to that proposed by Tachiya⁵² who pointed to the contradictory nature of the KM theory operating in terms of the parabolic energy surfaces with state dependent curvatures.

III. ELECTRON TRANSFER ACTIVATION ENERGY

ET reactions in polar fluids are capable of providing a crucial test of nonlinear solvation effects for at least two reasons. First, ET reactions are generally accompanied by creation of large ET dipole moments. Second, experimentally widely used sampling of the ET free energy gap gives information about the solute dipole dependence of the dipolar solvation energy inaccessible from usual optical experiments. Let us consider the latter point in more detail.

The key difference between the dipole solvation thermodynamics and ET kinetics is that the latter involves solvation of a nonequilibrium dipole m^\ddagger in the activated ET state. The value of m^\ddagger is chiefly determined by two factors: (i) the linear solvent response function or, in other words, the force constant along the ET reaction coordinate and (ii) the magnitude of the ET vacuum energy gap ΔE_0 . The variation of ΔE_0 changes in turn m^\ddagger . Therefore, by sampling ΔE_0 , we get in fact the variation of the effective dipole m^\ddagger and the solvation free energy $\mu_p(m^\ddagger)$ determining the activation barrier. Especially in the inverted region of ET m^\ddagger may deviate significantly from the equilibrium solute dipole moments. In this case nonlinear solvation effects may assume significance. This point becomes clearer when ET is treated in terms of a nonequilibrium solute dipole as the reaction coordinate.

We consider here the charge separation reaction $A-D \rightarrow A^- - D^+$ proceeding with changing the solute dipolar state $m_1 \rightarrow m_2$, $m_1 = 0$, $m_2 = \Delta m$. Widely accepted in the literature is a definition of the reaction coordinate X as the difference of the total energies of the donor and acceptor states^{33,38,40,53,54}

$$X = \Delta E_0 - \Delta m m \sum_j u_{0s}(0j),$$

where $u_{0s}(0j)$ is the interaction energy between the unitary solute and solvent dipoles, j denotes the orientation and the position of the j th solvent molecule, "0" refers to the solute, $\Delta E_0 = \hbar\Omega = E_{02} - E_{01}$, and E_{0i} are the vacuum energies of the donor-acceptor complex. For the reaction coordinate X , analogously to Eqs. (2) and (3), the diabatic free energy surfaces in the initial ($i=1$) and final ($i=2$) states are determined by the relation

$$\exp[-\beta F_i(X) + \beta E_{0i}] = \int_{-\infty}^{\infty} \frac{ds}{2\pi} \exp[is\beta(X - \Delta E_0) - \beta\mu_p(m_i + is\Delta m)]. \quad (12)$$

If we define the ET reaction coordinate through the effective solute dipole moment

$$d = \frac{\Delta E_0 - X}{2a\Delta m},$$

[a is the linear response coefficient $\mu_p(\Delta m) = -a\Delta m^2$], we get in the linear response approximation

$$F_1(d) = E_{01} + ad^2,$$

$$F_2(d) = E_{02} + a(d - \Delta m)^2 - a\Delta m^2.$$

The energies $F_i(d)$ are analogues of Marcus⁸ parabolas with the minima having the clear physical meaning of the solute dipole moments in the initial and final states. The ET problem can thus be formulated in terms of the nonequilibrium solute dipole d . Note that at this stage we do not assume the point character of the solute dipole. In this sense the formulation in terms of the solute dipole reaction coordinate is essentially analogous to that of Marcus through a charging parameter.²⁶ Furthermore, the theory, for the sake of consistency with our dipole solvation treatment, formulated for charge separation, is not actually restricted to this particular reaction. The description in terms of the d -coordinate remains intact for a more general case of charged reactants. However, for such systems, the solvation potential has to be calculated for the reference liquid perturbed by a charged solute.

For nonlinear solvation, the free energy surfaces can be evaluated by integrating over s in Eq. (12). Actually, we need to determine only one surface, since they are connected by the exact formula

$$F_2(d) = F_1(d) + \Delta E_0 - (2a\Delta m)d, \quad (13)$$

derived in Appendix A. Analogous relations in terms of the reaction coordinate X have been suggested previously in the literature.^{38,43}

The free energy $F_1(d)$ can be evaluated in a way similar to that in the preceding section, in the steepest-descent approximation, which proves to be very accurate compared to exact numerical integration. In this way, the diabatic ET free energy functions are given by the relations

$$F_1(d) = E_{01} + am^\ddagger d(1 - bm^{\ddagger 2}), \quad (14)$$

$$F_2(d) = E_{02} + am^\ddagger d(1 - bm^{\ddagger 2}) - (2a\Delta m)d, \quad (15)$$

where m^\ddagger is related to d by

$$\frac{m^\ddagger}{(1 + bm^{\ddagger 2})^2} = d.$$

The minima of $F_i(d)$ are located at the points

$$d_{\min}^{(1)} = 0, \quad d_{\min}^{(2)} = -\mu_p'(\Delta m)/(2a). \quad (16)$$

The latter relations are exact and independent of the particular form of $\mu_p(\Delta m)$ used.

Analogously to the spectroscopic formulation [Eq. (9)], the range of possible vacuum gaps at which the surfaces $F_i(d)$ have an intersection point is limited by the inequality $|\Delta E_0| \leq E_{\text{lim}}$ restricting by this means the accessible reaction coordinate values $|d| \leq 9/(16\sqrt{3}b)$. When ΔE_0 falls outside this range, the energy of dipolar fluctuations is not enough to surmount the barrier and the activation energy in the dipolar

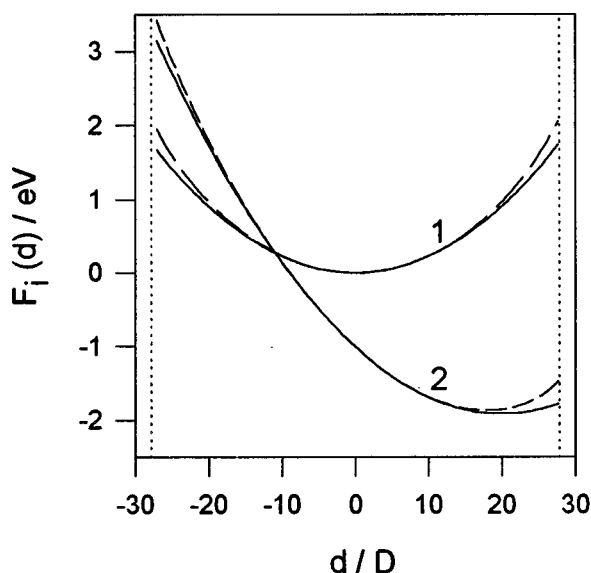


FIG. 4. Diabatic ET free energy surfaces along the reaction coordinate d for the charge separation (1) and charge recombination (2) reactions. The solid lines indicate nonlinear solvation, the dashed lines show the linear response results. The vertical dotted lines confine the range of accessible d -values at which intersection of $F_1(d)$ and $F_2(d)$ is possible. The solvent and solute parameters are: $\sigma=5$ Å, $\rho^*=0.955$, $m=2$ D, $R_0=4$ Å, $\Delta m=20$ D, $\Delta E_0=-1$ eV.

fluctuations channel becomes infinite. Other mechanisms of ET activation should be involved in this case for the reaction to proceed. The constraint imposed on the energy gap values seems to be the main qualitative consequence of nonlinear dipolar solvation. The deviation of the energy surfaces $F_i(d)$ from the linear response parabolic behavior is relatively small and doesn't exceed 20% at the boundaries of the permissible range of d 's (Fig. 4). Additionally, for exothermic ET reactions, the nonlinear solvation effect will be concealed by intramolecular vibrational excitations.

The ET reorganization energy cannot be defined in an unique way when nonlinear solvation is involved. We will determine therefore the solvent reorganization energies for each state through the corresponding vertical transition energies $\hbar\omega_{\text{abs}}$ and $\hbar\omega_{\text{fl}}$ ⁴²

$$\lambda_1 = \hbar\omega_{\text{abs}} - \Delta G, \quad \lambda_2 = \pm \hbar\omega_{\text{fl}} + \Delta G, \quad (17)$$

where “+” corresponds to the normal region of ET ($\Delta G < -\mu_p(\Delta m)$) and “-” to the spectroscopically more common case of $\Delta G > -\mu_p(\Delta m)$ ($\Delta E_0 > 0$). The vertical transition energies are given in this case by

$$\hbar\omega_{\text{abs}} = F_2(0) - F_1(0), \quad \hbar\omega_{\text{fl}} = |F_1(d_{\text{min}}^{(2)}) - F_2(d_{\text{min}}^{(2)})| \quad (18)$$

and $\Delta G = \Delta E_0 + \mu_p(\Delta m)$. From Eqs. (13), (16), (17), and (18) we get immediately

$$\lambda_1 = -\mu_p(\Delta m), \quad \lambda_2 = -\Delta m \mu'_p(\Delta m) + \mu_p(\Delta m). \quad (19)$$

For $\mu_p(\Delta m)$ given by Eq. (4),

$$\lambda_2 = \lambda_1 \frac{1 - b\Delta m^2}{1 + b\Delta m^2}$$

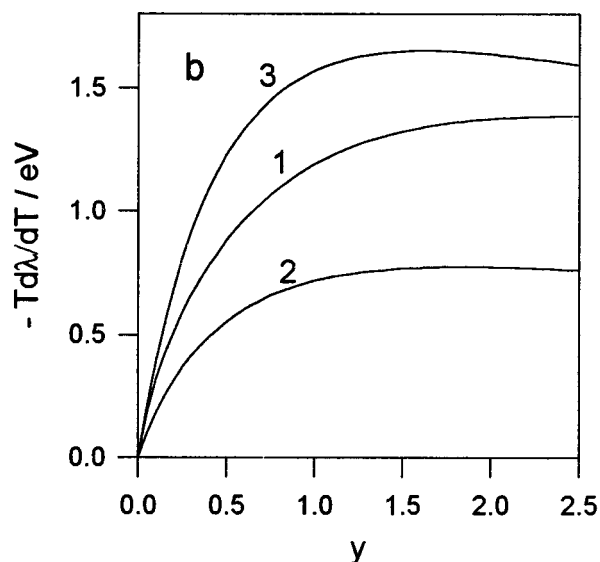
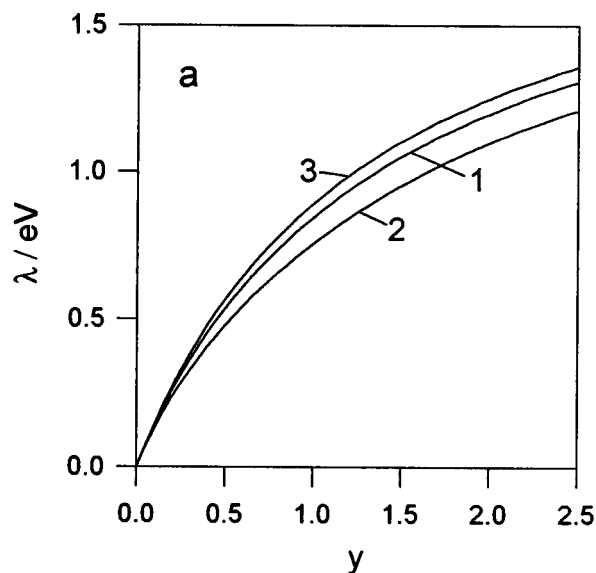


FIG. 5. Dependence of the reorganization energies (a) and their temperature derivatives (b) on the solvent dipolar density y . Numbers denote charge separation λ_1 (1), charge recombination λ_2 (2), and the linear response $\lambda^{(l)} = \lambda_1^2/\bar{\lambda}$, $\bar{\lambda} = (\lambda_1 + \lambda_2)/2$ (3) reorganization energies. The solvent and solute parameters are $\sigma=5$ Å, $\rho^*=0.955$, $R_0=4$ Å, $\Delta m=20$ D, $\alpha_p = 10^{-3}$ K⁻¹.

and the combination

$$\lambda^{(l)} = \lambda_1^2/\bar{\lambda}, \quad \bar{\lambda} = (\lambda_1 + \lambda_2)/2 \quad (20)$$

gives the linear response reorganization energy $\lambda^{(l)}$. This result offers a natural way of experimentally testing the nonlinear effects on reorganization energy by comparing λ_i to their combination (20). Further, due to the inequality $|\mu_p(\Delta m)| < a\Delta m^2$, the relation $\lambda_2 < \lambda_1$ should be universal as well. The difference between λ_2 and λ_1 is, however, rather modest ($\approx 15\%$, Fig. 5a) and is much smaller than the deviation of about 40% reported for dipolar lattice simulations by Zhou and Szabo.⁴² The difference in the nonlinearity effect seems to originate from the local solvent electrostriction occurring in fluids but excluded in lattice media. In liq-

uid media, the solvation power is decreased due to the local compression of the liquid compensating the effect of the alignment of the permanent dipoles.

The nonlinear solvation effect, moderate for reorganization energies, becomes more pronounced for their temperature derivatives (Fig. 5b) implying the ET entropy can be noticeably higher for charge separation than for charge recombination. The temperature derivatives of λ_1 and λ_2 have been calculated by accounting for the explicit temperature dependence in γ and the density variation as follows:

$$\rho = \rho(T_0)[1 - \alpha_p(T - T_0)], \quad T_0 = 298 \text{ K},$$

where α_p is the solvent isobaric expansibility. [The temperature variation of the solvent HS diameter may also be taken into account, but it produces no significant effect.] The physical reason for the higher sensitivity of the entropy to solvation nonlinearity is rooted in the fact that the entropy reflects the solvent configurational sensitivity to thermal excitations. The ability of the liquid to respond to the temperature increase becomes diminished by the nonlinear saturation of dipolar orientations making the liquid around the solute configurationally more rigid. Our reorganization energy calculations show, as a whole, a minor effect of nonlinearity on the free energy surfaces $F_p(d)$, in accord with some previous studies^{10,12,15,16,33} and in disagreement with others.^{21,42,43} The effect of nonlinearity on ET activation entropies has not been previously explored. The significant difference between the entropies of charge separation and charge recombination found in the present paper may offer an experimental way of testing nonlinear solvation theories.

Equation (19) gives an exact definition of the charge separation/recombination reorganization energies. It enables one to carry out a general thermodynamic analysis of solvent reorganization in terms of its enthalpy and entropy components. The reorganization energy of charge separation is just the negative of the chemical potential $\mu_p(\Delta m)$ of the ET dipole. It splits into the internal energy $u_p(\Delta m)$ and entropy $s_p(\Delta m)$ parts

$$\lambda_1 = -\mu_p(\Delta m) = -u_p(\Delta m) + Ts_p(\Delta m). \quad (21)$$

$\mu_p(\Delta m)$ can alternatively be defined as the free energy invested in charging the solute dipole m_0 from zero to Δm [see Eq. (2) of paper I]

$$\lambda_1 = -m \int_0^{\Delta m} dm_0 \int u_{0s}(01)g_{0s}(01;m_0)d\Gamma_1, \quad (22)$$

where $g_{0s}(01;m_0)$ is the solute-solvent pair distribution function for a solute with the dipole m_0 . We get from Eq. (22)

$$-\Delta m \mu'_p(\Delta m) = -u_p(\Delta m).$$

This implies that λ_2 in Eq. (19) is just the entropy of dipolar solvation

$$\lambda_2 = -Ts_p(\Delta m). \quad (23)$$

The reorganization energy $\bar{\lambda}$ which is the arithmetic mean of λ_1 and λ_2 is also equal to the half of the Stokes shift. The latter is the difference of the energies of two vertical transi-

tions which cannot include any variation of the entropy. In accordance with this physical picture we get from Eqs. (22) and (23) only the internal energy component

$$\bar{\lambda} = -u_p(\Delta m). \quad (24)$$

This shows that the three reorganization energies λ_1 , λ_2 and $\bar{\lambda}$, though close in magnitude (Fig. 5a), are not equivalent thermodynamically. This is in fact the reason for their different temperature variation (Fig. 5b). Note also that the combination of any two of Eqs. (21), (23), and (24) gives the entropy and enthalpy of equilibrium solvation from optical spectra. Both solvation enthalpies and entropies are mostly unavailable for dipolar solutes.⁵⁵ A spectroscopic analysis in terms of Eqs. (21)-(24) provides therefore a new way of extracting thermodynamic potentials of equilibrium dipolar solvation. A realistic analysis should however include the solute and solvent polarizabilities.

IV. COMPARISON TO SIMULATIONS AND EXPERIMENT

The two major manifestations of the nonlinear solvation effect on optical spectral lines obtained in the present treatment are the line narrowing and the switch of the line shift dependence on Δm from quadratic to linear. Although these features have been obtained here by applying the Padé form (4), they are quite general and are based solely on the saturation concept. As a matter of fact, both effects are just consequences of the restriction $-E_{\text{lim}} \leq \Delta E \leq E_{\text{lim}}$ imposed on the energy band of dipolar fluctuations. The line narrowing should therefore appear in any model including this feature. Similarly, the linear Δm dependence of the line shift is achieved at large Δm magnitudes for any functional form of the solvation chemical potential $\mu_p(m) = am^2f(m)$ with the asymptotics $f(m) \rightarrow 1$ at $m \rightarrow 0$ and $f(m) \propto 1/m^2$ at $m \rightarrow \infty$. This can be seen from the following reasoning. The energetic boundary of the solvent dipolar fluctuations E_{lim} is obtained from the simultaneous conditions of equality to zero of the first two derivatives of the function $\mathcal{F}(s) = -is\beta\Delta E - \beta\mu_p(\mathbf{m}_g + is\Delta\mathbf{m})$

$$\mathcal{F}'(s^\ddagger) = 0, \quad \mathcal{F}''(s^\ddagger) = 0.$$

The first condition gives

$$E_{\text{lim}} = a\Delta mm^\ddagger [2f(m^\ddagger) + m^\ddagger f'(m^\ddagger)]. \quad (25)$$

The second derivative \mathcal{F}'' is equal to $-2a\Delta m^2$ at low magnitudes of m and becomes positive at large m if for the expansion in the inverse m powers

$$\mu_p(m) = am^2f(m) = \sum_{i=0}^{\infty} \frac{a_i}{m^{2i}}$$

the condition $a_1 < 0$ is obeyed. As a result, \mathcal{F}'' passes through zero at some intermediate value of m^\ddagger independent of Δm and ΔE . Consequently, as is seen from Eq. (25), $E_{\text{lim}} \propto \Delta m$ (Fig. 3). From this consideration we can draw the conclusion that the general qualitative features of the nonlinear solvation effect are independent of the particular form of the solvation chemical potential involving the saturation

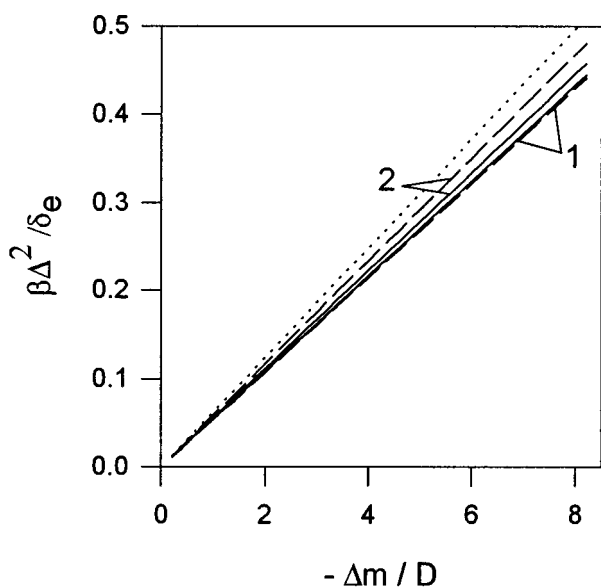


FIG. 6. The ratio $\beta\Delta^2/\delta_e$ vs $-\Delta m$ for the transition $m_g \rightarrow m_e$ with $m_g = 16.1$ D and m_e in the range from 16.1 to 7.85 D. The dotted line indicates the linear response result, the solid lines correspond to the nonlinear response of the dipolar fluid with $m = 1.69$ (1) and $m = 2.29$ (2) D according to the present theory. The dashed lines refer to the RHNC results with the solute and solvent parameters listed in the text.

limit. The prominence of the nonlinear effect depends, however, crucially on the magnitudes of the expansion coefficients a and b in Eq. (4). Our present calculations with $R_0 = 4$ Å indicate that deviations from linear behavior are substantial for emission lines with high values of the dipole moment variation $|\Delta m| \approx 15 - 20$ D. Although rather high, such magnitudes of Δm can be realized in spectroscopic applications, especially in molecular chromophores capable of intramolecular charge transfer.^{3,4,56,57} We will touch on comparison with experiment below and assess first the accuracy of the present calculations by comparing them with simulations.

Shemetulskis and Loring²⁸ performed Monte Carlo simulations of optical emission lines in dipolar liquids aimed at testing linear solvation theories. The nonlinear effect has been extracted from the deviation of the simulation data from the linear response relation between the width and the shift of the emission line

$$\beta\Delta^2/\delta_e = \Delta m^2/(\mathbf{m}_g \cdot \Delta \mathbf{m}). \quad (26)$$

The simulations were run for the dipolar fluid with the parameters $m = 1.69$ and 2.29 D, $\rho^* = 0.8$, and $\sigma = 4.3$ Å. For the chromophore, $R_0 = 3.85$ Å and $m_g = 16.1$ D were used. The validity of the relation (26) has been tested by varying the excited dipole moment m_e from 16.1 to 7.85 D, with \mathbf{m}_e parallel to \mathbf{m}_g . The simulation results were found to fall on the straight line as predicted by Eq. (26) but with a lower slope as the indication of the nonlinearity effect. The same picture is observed in the framework of the present theory. In Fig. 6, we have plotted the ratio (26) calculated from Eqs. (8) and (10) and from the reference hypernetted chain (RHNC) approximation shown previously⁵⁸ to be in good agreement

with the simulations of Shemetulskis and Loring.²⁸ As is seen in the figure, the two calculation schemes almost coincide for the dipolar solvent with $m = 1.69$ D. For the more polar solvent with $m = 2.29$ D both the RHNC approximation and simulations show the decrease of the nonlinearity effect reproduced by the Padé approximation. The extent of the nonlinearity decrease is, however, lower in the Padé form compared to the RHNC result. As was discussed in paper I, the RHNC calculation scheme restricted to the basis of 16 projections $h_{\alpha\beta}^{mnl}$ ($m, n \leq 2$; $\alpha, \beta = 0, s$) in the rotational-invariant expansion of the correlation function tends to underestimate the nonlinear effect at high solvent polarities leading to unphysically negative values of b coefficients in Eq. (4). It could also be that the Padé approximant becomes incorrect in this polarity range. Note also that the agreement between simulations²⁸ and the RHNC theory is not as close for $m = 2.29$ D as for $m = 1.69$ D solvent.

The nonlinear dependence of the band shift and width on the solute dipole variation Δm considered in the preceding section is difficult to test experimentally since such a test demands the accumulation of data for various chromophores. The chromophore change invokes in turn the solute size variation. This difficulty is surmounted by the observation that for commonly bulky chromophores the qualitative results concerning nonlinear effects on the spectral shift and width remain intact when they are plotted against $|\Delta m|/R_{0s}^{3/2}$ instead of $|\Delta m|$. However, the practical applicability of such tests is considerably diminished by the scarcity of reliable data on the solute dipole moments and sizes. Therefore, the solvent polarity dependence explored in most spectroscopic studies of solvent effects remains the main source of testing nonlinear solvation effects.

Equation (1) is a common probe of linear behavior. Although this viewpoint is widely adopted, it is generally unclear what type of deviations should the nonlinearity bring about. The present treatment predicts that for a transition with the solute dipole enhancement $m_e > m_g$ the emission bandwidth is lower than that of absorption

$$\Delta_e < \Delta_a.$$

The Stokes shift should also decrease compared to the linear response value due to the lower δ_e . As the consequence of these two factors, the absorption bandwidth deviates upward and emission bandwidth deviates downward from the Stokes shift (Fig. 7). In accord with this result, the inhomogeneous broadening was found to be substantially smaller in emission than in absorption for the coumarin-153 (C153) dye⁹ characterized by parameters: $m_g = 6.55$ D, $m_e \approx 15$ D, and $R_0 = 3.9$ Å. The plot of $\beta\Delta_a^2$ and $\beta\Delta_e^2$ vs the Stokes shift $\hbar\Delta\omega_{st} = \delta_e - \delta_a$ (Fig. 7) taken from experimental data for 40 nonpolar and polar solvents⁹ differs, however, from the trend shown in Fig. 7. The main feature seen in Fig. 8 is that $\beta\Delta_{a,e}^2$ are considerably higher than $\delta_e - \delta_a$. This is not unexpected if the intramolecular solute vibrations are taken into account. Eq. (1) actually holds only for classical solute and solvent modes. For quantum vibrations with the characteristic frequency ω_i , $\beta\hbar\omega_i \gg 2$ the spectral width is approximately determined by the relation⁴

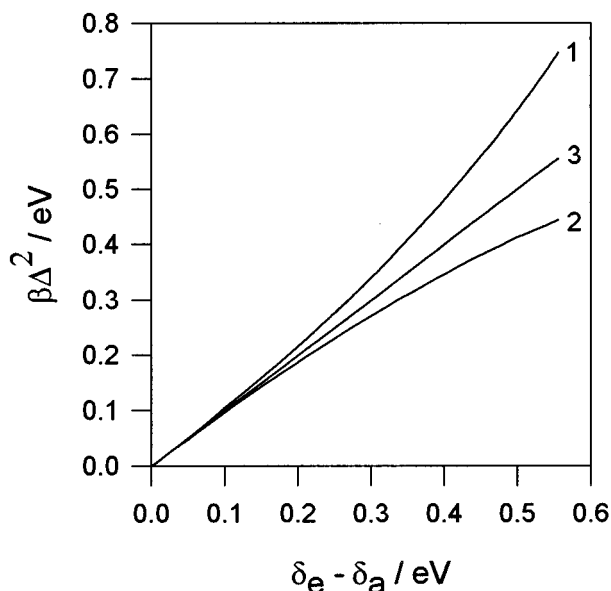


FIG. 7. Calculated absorption (1) and emission (2) widths vs the Stokes shift $\delta_e - \delta_a$. 3 shows the linear response prediction $\beta\Delta_{a,e}^2 = \delta_e - \delta_a$. The lines (1)-(3) are obtained by varying the solvent dipole moment in the range $0 \leq m \leq 4$ D with $\sigma = 4$ Å and $\rho^* = 0.859$. The solute parameters are those of coumarin-153: $m_g = 6.55$ D, $m_e = 15$ D, and $R_0 = 3.9$ Å.

$$\beta\Delta^2 \approx \hbar\Delta\omega_{st} + \lambda_i(\beta\hbar\omega_i - 2),$$

where λ_i is the reorganization energy of the solute intramolecular vibrations. Consequently, $\beta\Delta_{a,e}^2$ should become higher than $\hbar\Delta\omega_{st}$ under the influence of the solute quantum vibrations as is actually observed for C153. The participation of quantum vibrations in the bandwidth depends on the line shift and thus varies with the solvent. An accurate test of the

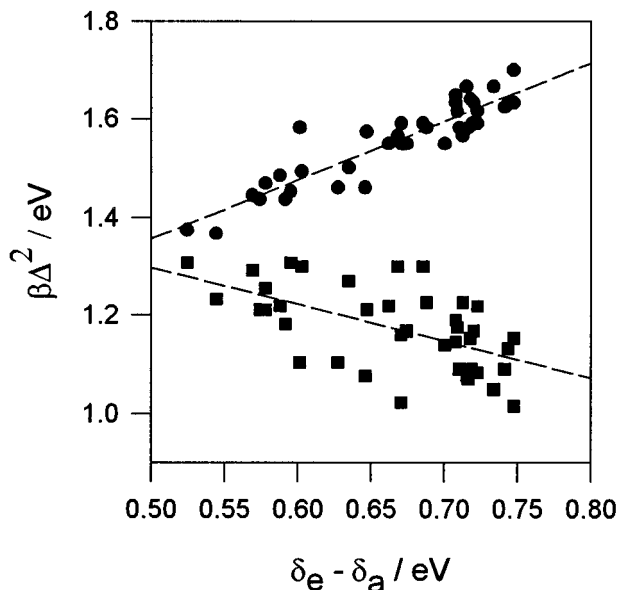


FIG. 8. Experimentally measured (Ref. 9) absorption (●) and fluorescence (■) widths vs the Stokes shift for coumarin-153 in 40 solvents. The dashed lines are the regressions drawn through the points. The solute parameters are as in Fig. 7.

linear theories by Eq. (1) demands therefore a bandshape analysis including quantum vibrational modes. In the absence of such data, a more direct verification of the LRA can be achieved in terms of the absorption and emission bandshifts.

In the LRA, the absorption and fluorescence energies can be represented by the relations

$$\begin{aligned} \hbar\omega_{\text{abs}} &= \hbar\omega_{0,\text{abs}} + \Delta E_{\text{disp}} - 2m_g(m_e - m_g)\Psi \\ &\quad - (m_e - m_g)^2\Psi^\infty, \\ \hbar\omega_{\text{fl}} &= \hbar\omega_{0,\text{fl}} + \Delta E_{\text{disp}} - 2m_e(m_e - m_g)\Psi \\ &\quad + (m_e - m_g)^2\Psi^\infty, \end{aligned}$$

where the gas phase absorption $\hbar\omega_{0,\text{abs}}$ and fluorescence $\hbar\omega_{0,\text{fl}}$ energies are shifted due to the differential dispersion solute-solvent coupling ΔE_{disp} . The response functions Ψ and Ψ^∞ correspond to the effect of the solvent permanent and induced dipoles, respectively. The solvatochromic behavior of C153 was found to be similar to that of the 4-nitroanisole dye⁹ used for constructing the π^* solvent polarity scale.² Because the dispersion component in 4-nitroanisole does not contribute substantially to the shift,³⁶ ΔE_{disp} is expected to be relatively small and weakly varying with solvent polarity also for C153. Therefore, the plot of

$$\hbar\tilde{\omega}_{\text{abs}} = \hbar\omega_{\text{abs}} + (m_e - m_g)^2\Psi^\infty \quad (27)$$

against

$$\hbar\tilde{\omega}_{\text{fl}} = \hbar\omega_{\text{fl}} - (m_e - m_g)^2\Psi^\infty \quad (28)$$

is expected to be linear with the slope $m_g/m_e = 0.437$ for C153. For the induction high-frequency component, the response function Ψ^∞ can be taken in the semicontinuum approximation³⁰

$$\Psi^\infty = \frac{1}{(R_0 + \sigma/2)^3} \frac{\epsilon_\infty - 1}{\epsilon_\infty + 2}, \quad (29)$$

where ϵ_∞ is the high-frequency solvent dielectric constant. The experimental⁹ absorption and fluorescence energies corrected according to Eqs. (27)-(29) are plotted in Fig. 9(a) for 25 solvents for which both experimental spectral data and hard sphere diameters⁴⁹ are available. The slope value of 0.51 of the regression line is higher than the LRA prediction in accordance with our expectation of the diminished fluorescence energy. Moreover, the calculation of the absorption and fluorescence shifts in the framework of the present theory for a model solvent with $\sigma = 4$ Å, $\eta = 0.45$, and the dipole moment in the range $0 \leq m \leq 4$ D yields for C153 the slope 0.53 very close to experiment [Fig. 9(a)]. Analogous results can be obtained for other dyes of the coumarin series.⁵⁹

Similarly high theory-experiment coincidence is achieved for the classical Lippert⁷ data on the fluorescence and absorption energies of 4-dimethylamino-benzene-4'-nitroaniline dye ($m_g = 8.6$ D, $m_e = 38$ D, and $R_0 = 8$ Å). Both the theory and experiment result in this case in the slope 0.226 [Fig. 9(b)] between the absorption and emission energies corresponding to the linear response prediction

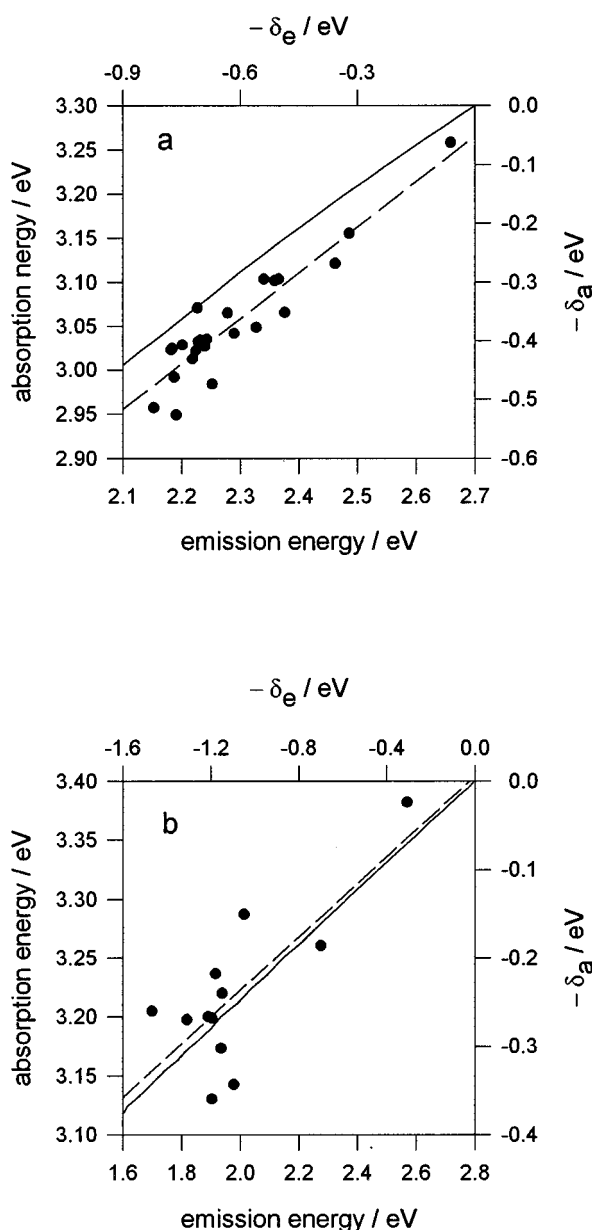


FIG. 9. Absorption energies of Eq. (27) vs fluorescence energies of Eq. (28) obtained from experimental data for coumarin-153 (Ref. 9) (a) and for 4-dimethylaminobenzene-4'-nitroaniline (Ref. 7) (b) dyes in a number of solvents (\bullet). The dashed regression lines have the slope 0.53 (a) and 0.227 (b). The solid lines show the dependence of the absorption vs fluorescence shift calculated in the present theory for a model solvent with $\sigma=4 \text{ \AA}$, $\rho^*=0.859$, and the dipole moment in the range $0 \leq m \leq 4 \text{ D}$. The slopes of the solid lines are 0.51 (a) and 0.226 (b). The solute parameters are as in Fig. 7.

m_g/m_e . The latter circumstance is due to the large chromophore size weakening the solute-solvent dipole-dipole coupling. The size effect may be also responsible for the higher scatter of the points in Fig. 9(b) due to an enhanced impact of the solvent-dependent dispersion term ΔE_{disp} .³⁰

V. SUMMARY

Almost all current studies of nonlinearity in solvation phenomena have addressed the question of the extent of de-

viation from the linear response predictions. In the present paper we approached the problem from a somewhat different standpoint. The question raised by the study is: If dipolar saturation manifests itself in dipole solvation, what would be the observable consequences for steady state spectroscopy and ET? We concentrated thus on qualitative insights into the effect of nonlinear dipole solvation on optical and radiationless transitions aimed at understanding the types of deviations from the linear response theories that should be expected. Since the bandwidth and the solvent-induced line shift are two spectral characteristics most commonly available from experiment, we focused on these two parameters. The main point of concern of our treatment is that deviations from linear behavior should be sought for transitions with high dipole moments in the initial state. This condition is most often realized for emission spectra. For absorption transitions $0 \rightarrow m_e$, no substantial nonlinear effects have been found, in accord with previous studies.^{15,24} As a result of the nonlinear solvation effect both the bandwidth and the spectral shift deflect downward from the linear response prediction. The dependence of the emission shift on the dye dipole variation Δm switches in the nonlinear region from the quadratic linear response trend $\propto \Delta m^2$ to the linear variation $\propto |\Delta m|$. The bandwidth in emission is predicted to be narrowed compared to the absorption width and even may pass through a maximum as a function of $|\Delta m|$. Ultimately, with increasing solvent polarity, the absorption width $\beta \Delta_a^2$ deviates upward and the emission width $\beta \Delta_e^2$ downward from the Stokes shift. Comparison of the theory predictions with simulations and experiment shows that it is generally in good quantitative agreement with the observed results.

The form of the linear behavior criterion is the issue of particular interest for spectroscopic applications. The criterion can be easily extracted from our analysis. The emission line shift may be treated according to the LRA if the linear shift $\delta_e^{(l)}$ doesn't reach the fluctuation band boundary: $|\delta_e^{(l)}| = 2am_e \Delta m \ll E_{\text{lim}}$. This yields the condition $m_e \ll 9/16 \sqrt{3b}$. For commonly bulky chromophores $R_0 > \sigma$ the criterion can be simplified further, since in this case $b = \beta^2 m^2 / 150R_{0s}^6$. We thus get that for the linear behavior to hold for an emission transition the inequality $\beta m_e m / R_{0s}^3 \ll 4$ should apply.

The solvent reorganization energy of intramolecular ET deserves special comment. As we have shown in Sec. IV, the width of emission (charge recombination) transition is lower than that of absorption (charge separation). Since the linewidth is commonly related to the reorganization energy (classical modes) by the expression $\Delta^2 = 2\lambda k_B T$, this is consistent with the trend $\lambda_2 < \lambda_1$ found for ET reactions. However, under a nonlinear description, different definitions of the reorganization energy no longer coincide and the values obtained from the vertical transition energetics differ from those from the linewidths. The reorganization energy loses thus its universal meaning of the strength of the coupling of the solute electron levels to the inertialess solvent fluctuations of condensed media. The width and shift need actually two separate characteristic parameters. This implies that when the nonlinear activation energy is fitted by the Marcus-

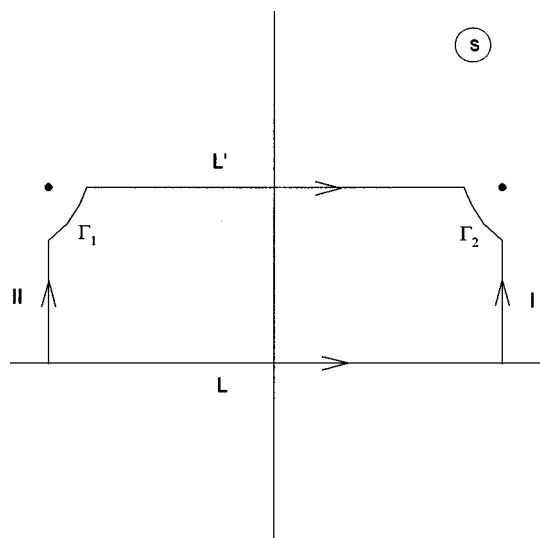


FIG. 10. Integration contour C. The two points indicate essential singularities of the integrand. The integrals over the semicircles Γ_1 and Γ_2 are equal to zero.

type quadratic form, it should contain two effective solvent reorganization energies.

Another important conclusion concerning ET follows from the comparison of the charge separation and charge recombination reorganization energies in Eq. (19). These expressions follow from exact relations (13) and (16) and are therefore independent of the particular form of the solvation chemical potential applied. It is seen that we can use simply the solvation chemical potential to calculate the nonlinear reorganization energy for charge separation but need a more complicated relation for charge recombination. This point is pertinent to the often used representation of the reorganization energy in terms of the solvation free energy which is thus restricted to linear response and charge separation reactions.

The substantial difference between the reorganization entropies of charge separation and charge recombination is an important outcome of the present study. This result offers a way of testing the nonlinear solvation theories from the thermochromism of optical spectra. Additionally, the thermodynamic distinctions between different definitions of the reorganization energy (21)-(24) yield enthalpies and entropies of equilibrium solvation from optical absorption and fluorescence energies.

ACKNOWLEDGMENT

This work has been supported by Grant No. CHE-9520619 from the National Science Foundation. It was presented at the Rocky Mountain ACS Regional Meeting in Denver, CO (June 11, 1996).

APPENDIX A: CONNECTION BETWEEN F_1 AND F_2

The free energy surface of the charge separated state is determined by the relation

$$I_L = \exp[-\beta F_2(d) + \beta E_{02}] = \text{Re} \int_L \frac{ds}{2\pi} \exp[\mathcal{F}_2(s)],$$

where the integration is performed over the segment L: $-1/\sqrt{b} \leq s \leq 1/\sqrt{b}$ and

$$\mathcal{F}_2(s) = -i(2\beta\Delta md)s - \beta\mu_p(\Delta m(1 + is)).$$

Since the integrand is analytic inside the closed contour C shown in Fig. 10, we get

$$I_C = \text{Re} \int_C \frac{ds}{2\pi} \exp[\mathcal{F}_2(s)] = 0.$$

The contour integral is represented by the sum of the constituents

$$I_C = I_L + I_I - I_{II} - I_{L'} \quad (\text{A1})$$

over the contour parts depicted in Fig. 10. It is easy to show that $I_I - I_{II}$ is the difference of complex conjugate values giving no contribution to the real value of the integral. For the integral $I_{L'}$, the variable change $s = i + t$ immediately gives

$$I_{L'} = \exp[\beta(E_{01} + 2a\Delta md - F_1(d))],$$

which combined with Eq. (A1) results in Eq. (13).

- ¹Y. Marcus, Chem. Soc. Rev. 403 (1993).
- ²C. Reichardt, Chem. Rev. 94, 2319 (1994).
- ³G. C. Walker, E. Åkesson, A. E. Johnson, N. E. Levinger, and P. F. Barbara, J. Phys. Chem. 96, 3728 (1992); I. R. Gould, D. Noukakis, J. L. Goodman, R. H. Young, and S. Farid, J. Am. Chem. Soc. 115, 3830 (1993).
- ⁴J. Cortés, H. Heitele, and J. Jortner, J. Phys. Chem. 98, 2527 (1994).
- ⁵D. V. Matyushov and B. M. Ladanyi, J. Chem. Phys. 107, 1362 (1997), preceding paper. (This is referred to as paper I in the text.)
- ⁶N. S. Bayliss and E. G. McRae, J. Phys. Chem. 58, 1002 (1954); E. Lippert, Z. Naturforsch. Teil A 10, 541 (1955); N. Mataga, Y. Kaifu, and M. Koizumi, Bull. Chem. Soc. Jpn. 28, 690 (1955); 29, 465 (1956); W. Liptay, Z. Naturforsch. Teil A 20, 1441 (1965).
- ⁷E. Lippert, Z. Electrochem. 61, 962 (1957).
- ⁸R. A. Marcus, J. Chem. Phys. 43, 1261 (1965).
- ⁹M. L. Horng, J. A. Gardecki, A. Papazyan, and M. Maroncelli, J. Phys. Chem. 99, 17311 (1995).
- ¹⁰H.-A. Yu and M. Karplus, J. Chem. Phys. 89, 2366 (1988).
- ¹¹P. G. Kusalik and G. N. Paty, J. Chem. Phys. 89, 5843 (1988).
- ¹²R. A. Kuharski, J. S. Bader, D. Chandler, M. Sprik, M. L. Klein, and R. W. Impey, J. Chem. Phys. 89, 3248 (1988).
- ¹³E. A. Carter and J. T. Hynes, J. Phys. Chem. 93, 2184 (1989).
- ¹⁴M. Maroncelli and G. R. Fleming, J. Chem. Phys. 89, 5044 (1988).
- ¹⁵M. Maroncelli, J. Chem. Phys. 94, 2084 (1991).
- ¹⁶T. Fonseca, B. M. Ladanyi, and J. T. Hynes, J. Phys. Chem. 96, 4085 (1992).
- ¹⁷E. A. Carter and J. T. Hynes, J. Chem. Phys. 94, 5961 (1991).
- ¹⁸T. Fonseca and B. M. Ladanyi, J. Phys. Chem. 95, 2116 (1991); T. Fonseca and B. M. Ladanyi, in *Ultrafast Reaction Dynamics and Solvent Effects*, edited by Y. Gauduel and P. J. Rossky (AIP Press, New York, 1994).
- ¹⁹T. Fonseca and B. M. Ladanyi, J. Mol. Liq. 60, 1 (1994); M. S. Skaf and B. M. Ladanyi, J. Mol. Struct. (Theochem) 99, 553 (1995).
- ²⁰B. Jayaram, R. Fine, K. Sharp, and B. Honig, J. Phys. Chem. 93, 4320 (1989).
- ²¹Y. Hatano, M. Saito, T. Kakitani, and N. Mataga, J. Phys. Chem. 92, 1008 (1988); M. Saito and T. Kakitani, Chem. Phys. Lett. 172, 169 (1990).
- ²²A. Chandra and B. Bagchi, J. Chem. Phys. 99, 553 (1993).
- ²³J. Åqvist and T. Hansson, J. Phys. Chem. 100, 9512 (1996).
- ²⁴F. O. Raineri, H. Resat, B.-C. Perng, F. Hirata, and H. L. Friedman, J. Chem. Phys. 100, 1477 (1994).
- ²⁵P. V. Kumar and M. Maroncelli, J. Chem. Phys. 103, 3038 (1995).

- ²⁶R. A. Marcus, *J. Chem. Phys.* **24**, 966 (1956).
- ²⁷R. F. Loring, *J. Phys. Chem.* **94**, 513 (1990).
- ²⁸N. E. Shemetulskis and R. F. Loring, *J. Chem. Phys.* **95**, 4756 (1991).
- ²⁹D. V. Matyushov and R. Schmid, *Mol. Phys.* **84**, 533 (1995).
- ³⁰D. V. Matyushov and R. Schmid, *J. Chem. Phys.* **103**, 2034 (1995).
- ³¹J. S. Bader and B. J. Berne, *J. Chem. Phys.* **104**, 1293 (1996); F. J. Luque, J. M. Bofil, and M. Orozco, *ibid.* **103**, 10183 (1995); H. J. Kim, *ibid.* **105**, 6818 (1996).
- ³²B. D. Bursulaya, D. A. Zichi, and H. J. Kim, *J. Phys. Chem.* **99**, 10069 (1995); B. D. Bursulaya, D. A. Zichi, and H. J. Kim, *ibid.* **100**, 1392 (1996); B. D. Bursulaya and H. J. Kim, *ibid.* **100**, 16451 (1996); H. J. Kim, *J. Chem. Phys.* **105**, 6833 (1996).
- ³³G. King and A. Warshel, *J. Chem. Phys.* **93**, 8682 (1990).
- ³⁴G. Rauhut, T. Clark, and T. Steinke, *J. Am. Chem. Soc.* **115**, 9174 (1993); E. Leontidis, U. W. Suter, M. Schütz, H.-P. Lüthi, A. Renn, and U. P. Wild, *ibid.* **117**, 7493 (1995).
- ³⁵D. V. Matyushov, *Chem. Phys.* **211**, 47 (1996).
- ³⁶D. V. Matyushov, R. Schmid, and B. M. Ladanyi, *J. Phys. Chem.* **101**, 1035 (1997).
- ³⁷J. G. Saven and J. L. Skinner, *J. Chem. Phys.* **99**, 4391 (1993).
- ³⁸B.-C. Perng, M. D. Newton, F. O. Raineri, and H. L. Friedman, *J. Chem. Phys.* **104**, 7177 (1996); **104**, 7205 (1996).
- ³⁹R. Reynolds, J. A. Gardecki, S. J. V. Frankland, M. L. Horng, and M. Maroncelli, *J. Phys. Chem.* **100**, 10337 (1996).
- ⁴⁰A. Warshel, *J. Phys. Chem.* **86**, 2218 (1982); A. Warshel and W. W. Parson, *Annu. Rev. Phys. Chem.* **42**, 279 (1991).
- ⁴¹T. Kakitani, N. Matsuda, A. Yoshimori, and N. Mataga, *Prog. Reaction Kinetics* **20**, 347 (1995).
- ⁴²H.-X. Zhou and A. Szabo, *J. Chem. Phys.* **103**, 3481 (1995).
- ⁴³Y. Georgievskii, *J. Chem. Phys.* **104**, 5251 (1996).
- ⁴⁴A. M. Kjaer and J. Ulstrup, *J. Am. Chem. Soc.* **109**, 1934 (1987); M. Bixon, J. Jortner, J. Cortes, H. Heitele, and M. E. Michel-Beyerle, *J. Phys. Chem.* **98**, 7289 (1994).
- ⁴⁵A. I. Burstein, *J. Chem. Phys.* **103**, 7927 (1995).
- ⁴⁶P. H. Fries and G. N. Patey, *J. Chem. Phys.* **82**, 429 (1985).
- ⁴⁷M. S. Skaf and B. M. Ladanyi, *J. Chem. Phys.* **102**, 6542 (1995).
- ⁴⁸The dipolar liquid with parameters of methanol is however quite different from more realistic models. Equilibrium solvation in methanol is much more strongly nonlinear than one would expect for the “dipolar methanol” considered here. See the second entry of Ref. 18.
- ⁴⁹R. Schmid and D. V. Matyushov, *J. Phys. Chem.* **99**, 2393 (1995).
- ⁵⁰B. M. Ladanyi and R. M. Stratt, *J. Phys. Chem.* **100**, 1266 (1996).
- ⁵¹S.-H. Chong and F. Hirata, *J. Chem. Phys.* **106**, 5225 (1997).
- ⁵²M. Tachiya, *Chem. Phys. Lett.* **159**, 505 (1989).
- ⁵³M. Lax, *J. Chem. Phys.* **20**, 1752 (1952).
- ⁵⁴M. Tachiya, *J. Phys. Chem.* **93**, 7050 (1989).
- ⁵⁵A. Ben-Naim and Y. Marcus, *J. Chem. Phys.* **81**, 2016 (1984).
- ⁵⁶J. F. Létard, R. Lapouyade, and W. Rettig, *J. Am. Chem. Soc.* **115**, 2441 (1993); H. Ephardt and P. Fromherz, *J. Phys. Chem.* **95**, 6792 (1991); M. J. Foley and L. A. Singer, *ibid.* **98**, 6430 (1994).
- ⁵⁷R. M. Hermant, N. A. C. Bakker, T. Scherer, B. Krijnen, and J. W. Verhoeven, *J. Am. Chem. Soc.* **112**, 1214 (1990).
- ⁵⁸B. M. Ladanyi, N. F. Shemetulskis, and R. F. Loring, *J. Chem. Phys.* **96**, 8637 (1992).
- ⁵⁹K. Rechthaler and G. Köhler, *Chem. Phys.* **189**, 99 (1994).